Holography for Quantum Quenches
(Thermalization after holographic bilocal quench)

Irina Aref'eva

joint works with M. A. Khramtsov and M. D. Tikhanovskaya,
arXiv:1604.08905, arXiv:1706.07390
D.S. Ageev, arXiv:1701.07280, 1704.07747

Steklov Mathematical Institute, Russian Academy of Sciences

M$\cup\Phi$, Belgrade, 2017

Plan

- Introduction
- Thermalization after holographic bilocal quench
- Thermalization after global quench in thermal media
- Conclusion [comparison of local/global quenches]

Introduction. Thermalization in a quantum system

Thermalization in a quantum system is a major theoretical challenge. It is involved in many problems of physics (and not only) which involve initial states which are out of equilibrium:

- Early Universe
- Heavy ion collisions
- Dynamics of cold atomic gas
- etc.

Introduction. Thermalization/equilibration after quantum quench

A natural setup to study thermalization in *closed* quantum systems is **quantum quench**:

- Quantum system with a Hamiltonian H;
- At time t = 0, the Hamiltonian parameter is changed abruptly $H \to H'$ and $H'|\psi'\rangle = E|\psi'\rangle$
- for times $t > 0$ system evolves with H, and $|\psi(t)\rangle = \mathrm{e}^{-iH_2 t}|\psi'\rangle$.

Let A be a subsystem, with density matrix $\rho_A(t) = \mathrm{Tr}_{\bar{A}}|\psi(t)\rangle\langle\psi(t)|$

$\bar{A}$ - complement of A

The system **thermalizes**, if for any subsystem A it is true that

$$\lim_{T\to\infty} \frac{1}{T}\int_0^T \rho_A(t)dt = \rho_\beta = \frac{1}{Z}\mathrm{e}^{-\beta H_2} \quad \text{for some } \beta\,;$$

How do we probe it?

- Entanglement entropy: $S(A) = -\mathrm{Tr}_A\, \rho_A \log \rho_A$ - our primary tool
- More "fine-grained" observables: Renyi entropies, correlation functions of specific operators, ...

Quenches in CFT

CFT is a convenient arena to study quench dynamics (Cardy, Calabrese,'05)

- **Global quench** - excites every point of the circle uniformly in the initial state - **popular setup for studies of thermalization**:
  V. Balasubramanian et al, arXiv:1012.4753; E. Lopez et al, arXiv:1006.4090; Liu, Suh - arXiv:1305.7244, etc.
- **Local quench**: excites a point of the circle in the initial state
- **Bilocal quench**: excites two antipodal points (AKT: 1706.07390)

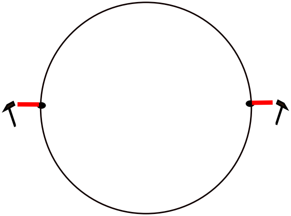

Bilocal quench

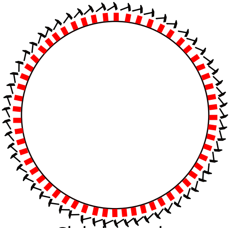

Global quench

The main goal of our work is to study the non-equilibrium dynamics of entanglement during thermalization after the bilocal quench in $(1+1)$d CFT on a cylinder using the holographic duality.

The bulk dual of the bilocal quench

- Local excitations in the boundary CFT_2 produce massless particles in the bulk $\Rightarrow$
  The holographic dual is the AdS_3 spacetime with two colliding massless point particles.
- We are interested in thermalization $\Rightarrow$ we study the case when the colliding particles **produce a black hole**.

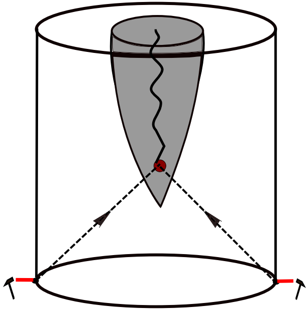

The AdS$_3$ spacetime

- a hyperboloid in the 4D flat space: $x_0^2 + x_3^2 - x_1^2 - x_2^2 = 1$
  Parametrize the hyperboloid by global coordinates:

$$x_3 = \cosh\chi \cos t, \quad x_0 = \cosh\chi \sin t, \quad x_1 = \sinh\chi \cos\phi, \quad x_2 = \sinh\chi \sin\phi$$

  where $\chi \in \mathbb{R}_+$, $t \in [-\pi, \pi]$, $\phi \in [0, 2\pi]$. The metric is

$$ds^2 = -\cosh^2\chi\, dt^2 + d\chi^2 + \sinh^2\chi\, d\phi^2$$

- $SL(2,\mathbb{R})$ group manifold:

$$X = \begin{pmatrix} x_3 + x_2 & x_0 + x_1 \\ x_1 - x_0 & x_3 - x_2 \end{pmatrix}, \qquad \det X = x_0^2 + x_3^2 - x_1^2 - x_2^2 = 1$$

- solution of vacuum 3D Einstein equations with negative cosmological constant

Identification isometries: $X \to X^* = \mathbf{u}^{-1} X \mathbf{u}$; $\mathbf{u}$ - *holonomy of the defect*

Massless particle in AdS_3

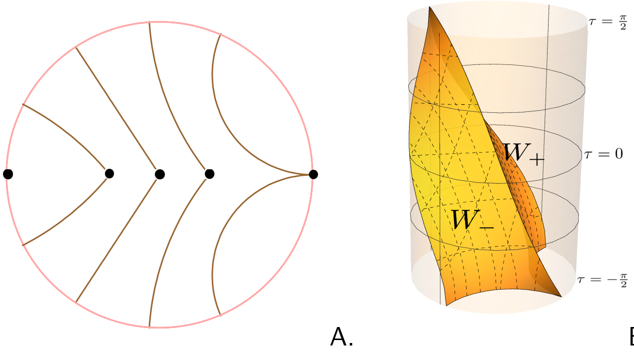

Figure: The identification of the massless particle.

The holonomy is: $\mathbf{u}_{\text{massless}} = \mathbf{1} + p^\mu \gamma_\mu$; (Matschull, gr-qc/9809087)
where

$$\mathbf{1} = \begin{pmatrix} 1 & 0 \\ 0 & 1 \end{pmatrix}, \quad \gamma_0 = \begin{pmatrix} 0 & 1 \\ -1 & 0 \end{pmatrix}, \quad \gamma_1 = \begin{pmatrix} 0 & 1 \\ 1 & 0 \end{pmatrix}, \quad \gamma_2 = \begin{pmatrix} 1 & 0 \\ 0 & -1 \end{pmatrix},$$

BTZ black hole in global AdS$_3$

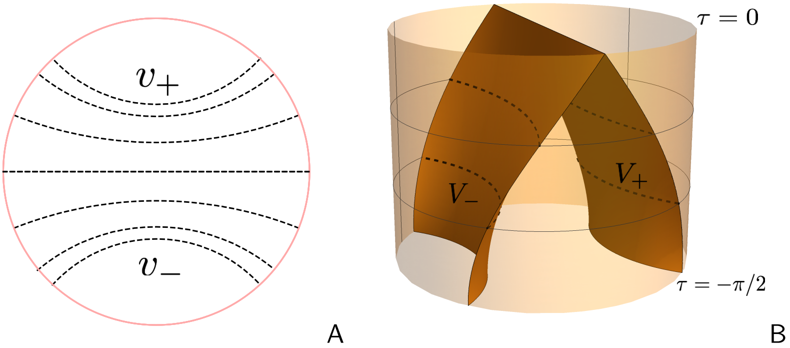

Figure: The maximally extended BTZ black hole in global coordinates.

Holonomy: $\mathbf{u}_{\mathrm{BTZ}} = \begin{pmatrix} -\cosh\mu & \sinh\mu \\ \sinh\mu & -\cosh\mu \end{pmatrix}$; where $\mu = \pi R$ - mass of BH

Collision of particles in the center of mass frame

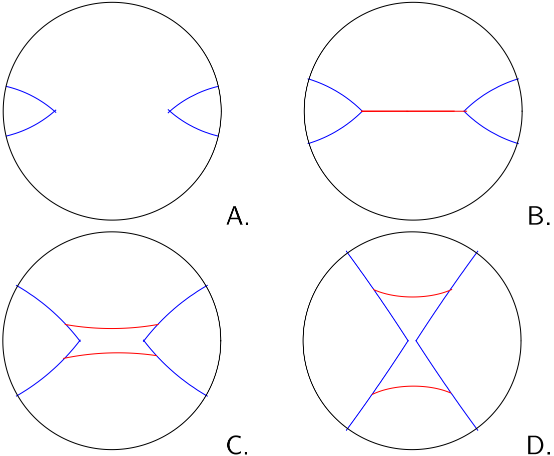

Collision of massless particles in the BTZ rest frame

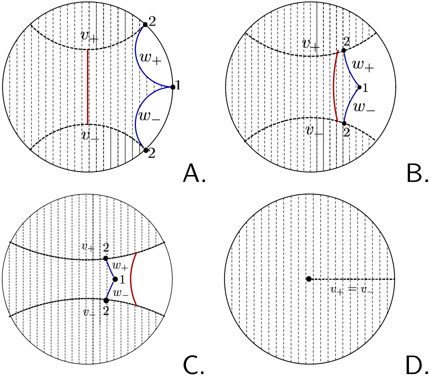

Figure: Collision of particles in the BTZ rest frame, Matschull

$$ds^2 = -\cosh^2\chi\, dt^2 + d\chi^2 + \sinh^2\chi\, d\phi^2$$

Identified surfaces:

$W_\pm$: $\tan\chi(\mathcal{E}\cos\phi \pm \sin\phi) = -\mathcal{E}\sin\tau\,,\ \mathcal{E} = \coth\frac{R\pi}{2}$

$V_\pm$:

$$\tanh\chi\sin\phi = \mp\sin t\tanh\pi R$$

Black hole creation in BTZ coordinates

To do the holographic computation, we need to map this quotient of global AdS_3 to an asymptotically AdS_3 spacetime with cylindrical boundary.
For this, we make transition to BTZ-Schwarzshild coordinates:

$$\begin{aligned}
x_0 = \cosh\chi \sin\tau &= -\frac{r}{R}\cosh R\ \varphi \\
x_2 = \sinh\chi \sin\phi &= \frac{r}{R}\sinh R\ \varphi \\
x_3 = \cosh\chi \cos\tau &= \sqrt{\frac{r^2}{R^2}-1}\sinh R\ t \\
x_1 = \sinh\chi \cos\phi &= \sqrt{\frac{r^2}{R^2}-1}\cosh R\ t
\end{aligned}$$

The metric has the form $ds^2 = -(r^2 - R^2)\ dt^2 + \frac{dr^2}{r^2-R^2} + r^2 d\varphi^2$, where $r > R$, $\varphi \in \mathbb{R}$, $t \in [0, +\infty)$.
What happens to the identification?

Black hole creation in BTZ coordinates

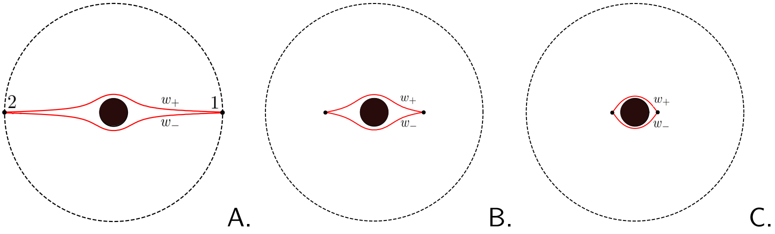

Figure: Cartoon of black hole creation in BTZ coordinates (A. Jevicki, J.Thaler, hep-th/0203172). **A**: particles start from the boundary at $t = 0$. **B**: Particles move through the bulk towards each other. **C**: Particles asymptotically approach the horizon.

$ds^2 = -(r^2 - R^2)\, dt^2 + \frac{dr^2}{r^2 - R^2} + r^2 d\varphi^2\,,$
Identified surfaces:

$$W_\pm : \quad \tanh\chi \frac{\sin\phi}{\sin\tau} = -\tanh R\varphi\,;$$
$$V_- \sim V_+ \;\Leftrightarrow\; \varphi \sim \varphi + 2\pi\,.$$

Two coordinate systems

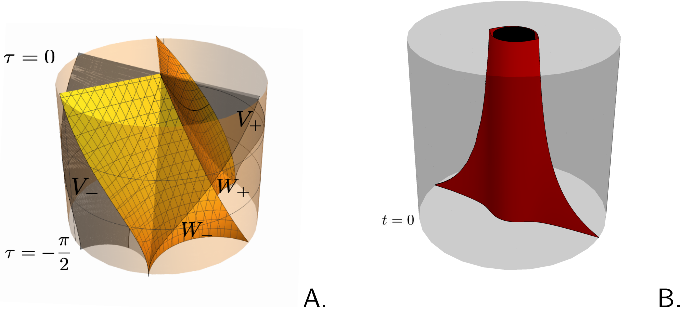

Figure: **A**. 3D picture of identification surfaces in global AdS_3. **B**. Creation of the black hole by colliding particles in BTZ coordinates. Red surfaces are the faces of identification $W_{\pm}$.

Holographic entanglement entropy

The entanglement entropy of a subsystem on a spatial subregion A in the boundary theory is calculated according to the formula
(Ryu, Takayanagi, hep-th/0603001;
Hubeny, Rangamani, Takayanagi (HRT), arXiv:0705.0016):

$$S(A) = \frac{\mathcal{A}}{4G}\,; \tag{1}$$

where $\mathcal{A}$ is the minimal area of a co-dimension 2 extremal surface in the bulk which has the same boundary as A and is homologous to A.
$\mathbf{AdS_3/CFT_2}$ case. In $d = 2$ $A = [a,\ b]$ is a segment of the circle. To calculate HEE, one has to find the minimal geodesic between equal-time points a and b on the boundary and calculate its length:

$$S(a,\ b) = \frac{\mathcal{L}_{\mathrm{min}}(a,\ b)}{4G}\,; \qquad \text{where } G = \frac{3}{2c}\,.$$

HRT geodesics

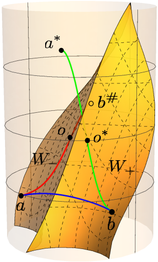

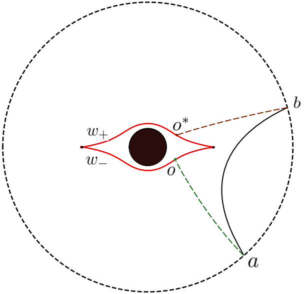

Denote

$$\Delta t = t_b - t_a\,; \quad t_0 = \tfrac{1}{2}(t_b + t_a)\,; \quad \Delta\varphi = \varphi_b - \varphi_a\,; \quad \varphi_0 = \tfrac{1}{2}(\varphi_b + \varphi_a)\,;$$

- **Direct geodesics** do not go through identification surfaces $W_\pm$.
- **Crossing geodesics** go through the identification surfaces $W_\pm$.

HRT geodesics and equilibration of entanglement

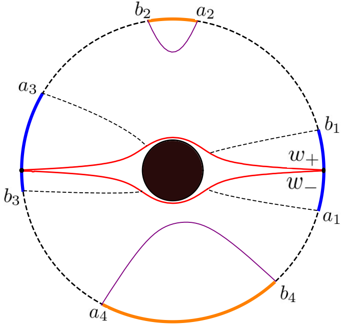

Two patterns of entanglement:

(*i*) HEE is constant for orange segments with φ_a, $\varphi_b \in [-\pi, 0)$, or φ_a, $\varphi_b \in [0, \pi)$

(*ii*) HEE grows with time up to thermal value for blue segments with $\varphi_a \in [-\pi, 0)$, and $\varphi_b \in [0, \pi)$:

Denote $\Delta\varphi = \varphi_b - \varphi_a$, $\varphi_0 = \frac{1}{2}(\varphi_a + \varphi_b)$.

Holographic entanglement entropy: results

- Static thermal equilibrium regime: direct geodesic dominates.

$$S_{\text{eq}}(a,\ b) = \frac{c}{3}\log\left(\frac{2}{\epsilon}\sinh\left(R\frac{\Delta\varphi}{2}\right)\right) \ ;$$

  This is thermal HEE.

- Dynamic non-equilibrium regime: crossing geodesic dominates.

$$S_{\text{non-eq}}(a,\ b|t) = \frac{c}{6}\log\left[\frac{2}{\epsilon}\left(-1+\mathcal{E}^2+(1+\mathcal{E}^2)\cosh R\Delta\varphi + \right.\right.$$
$$+\mathcal{E}^2\cosh 2R\varphi_0 + \mathcal{E}^2\cosh 2Rt - 2\mathcal{E}\sinh R\Delta\varphi +$$
$$\left.\left. +4\mathcal{E}\cosh Rt\cosh R\varphi_0\left(\sinh R\frac{\Delta\varphi}{2} - \mathcal{E}\cosh R\frac{\Delta\varphi}{2}\right)\right)\right] \ .$$

For $\varphi_0 = 0$: symmetry between t and $\frac{\Delta\varphi}{2}$

Evolution of entanglement entropy

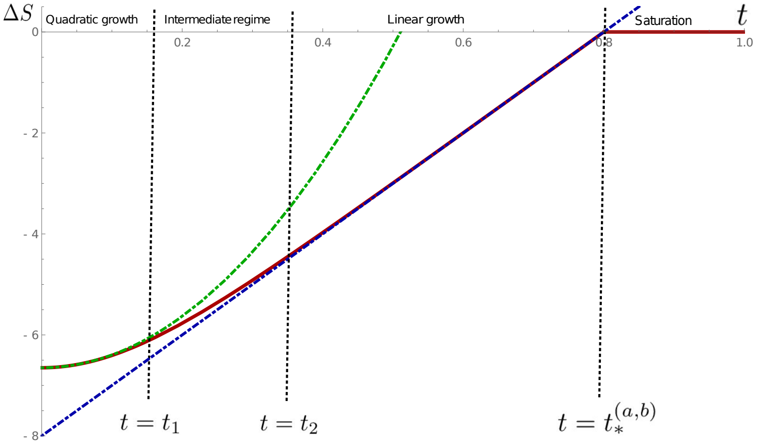

Figure: Here red curve is the function $\Delta S(t) = S_{\text{non-eq}}(t) - S_{\text{eq}}$, green dashed curve is the quadratic approximation, and blue dashed line is the linear asymptotic. **Main feature - sharp transition to saturation**.

Evolution of entanglement entropy ["global heating up"]

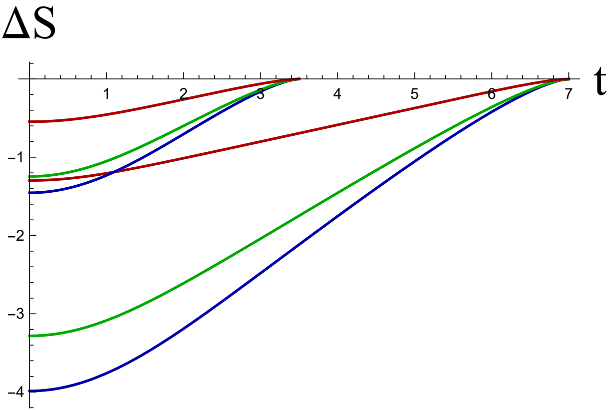

Figure: Here $\Delta S(t) = S_{\text{non-eq}}(t) - S_{\text{eq}}$, blue: $z_H = \infty, z_h = 1$; green $zH = 2.5, zh = 1$; red $zH = 1.3, zh = 1$. Top curves correspond to $\ell = 7$ and bottom ones to $\ell = 3.5$. **Main feature - smooth transition to saturation**.

Liu, Suh - arXiv:1305.7244, I.A., Ageev, 1701.07280

Time scales of entanglement equilibration

- "Pre-local equilibration time" $t = t_1 = \frac{\Delta\varphi}{2R}$ (H.Liu, S.Suh,1305.7244; I.A., D.Ageev, 1704.07747, in the global quench context)
- Crossing the apparent horizon: $t = t_2$
- Thermalization time $t = t_*^{(a,b)}$ - HEE saturates

$$\cosh R\ t_*^{(a,b)} = \cosh R\varphi_0 \left(\cosh R\frac{\Delta\varphi}{2} - \frac{1}{\mathcal{E}}\sinh R\frac{\Delta\varphi}{2}\right)$$

$$+\sqrt{\cosh^2 R\varphi_0 \left(\cosh R\frac{\Delta\varphi}{2} - \frac{1}{\mathcal{E}}\sinh R\frac{\Delta\varphi}{2}\right)^2 - \cosh^2 R\varphi_0 - \sinh^2 R\frac{\Delta\varphi}{2} + \frac{1}{\mathcal{E}}\sinh R\Delta\varphi}$$

Unlike the global quench case, we have **sharp transition** to saturation

Evolution of entanglement entropy

1. **Early-time quadratic growth**: $t < t_1$

$$S_{\text{non-eq}}(a,\ b|t) = S_{\text{non-eq}}(a,\ b|0) + f(\varphi_a, \varphi_b)\ t^2 + O(t^4)\,;$$

2. **Intermediate regime**: $t_1 \leq t < t_2$. Interpolation between quadratic and linear growth
3. **Linear growth**: $t_2 \leq t < t_*$

$$\Delta S(t) = S_{\text{non-eq}} - S_{\text{eq}} = \frac{c}{3} R\ t + \frac{c}{3} \log\left(\frac{\coth\frac{\pi R}{2}}{8\sinh^2 R\frac{\Delta\varphi}{2}}\right) + O(\mathrm{e}^{-Rt})\,.$$

4. **Saturation**: $t \geq t_*$. HEE is at thermal value.

Universality of entanglement growth

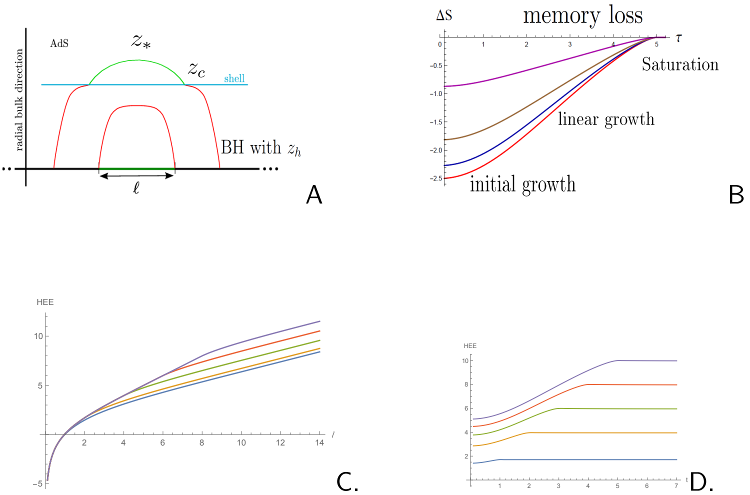

Figure: **A**: A: The shell in the BH background; **B**: $\Delta(t,\ell)S$;**C**: The holographic entanglement entropy $S(t,\ell)$ as function on t for given ℓ; **D**: $S(t,\ell)$ as function on ℓ for given t.

Memory loss and entanglement tsunami [bilocal quench]

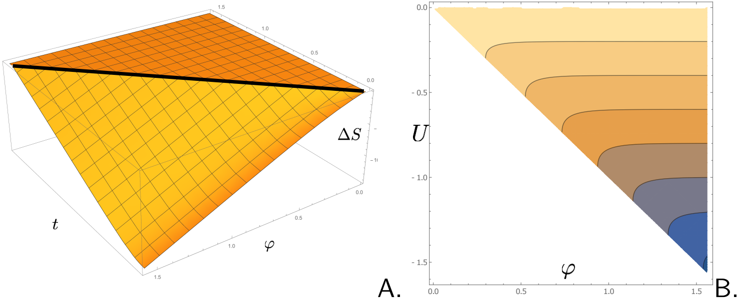

Figure: **A**: Entanglement spreading in case of symmetric intervals. The horizontal plateau represents the equilibrium regime. **B**: Density plot of non-equilibrium HEE as a function of $\varphi = \frac{\Delta\varphi}{2}$ and $U = t - \varphi$, with $R = 5$.

Tsunami=wave character=$S(\ell, t) = S(\ell - t)$

Memory loss and entanglement tsunami [global heating up]

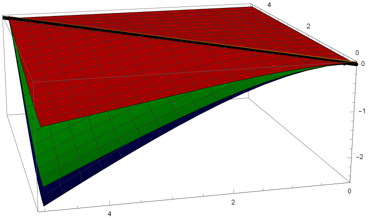

A.

Figure: 3D plot for $\Delta S(t,\ell)$ for the global heating up.

Linear growth and black hole interior

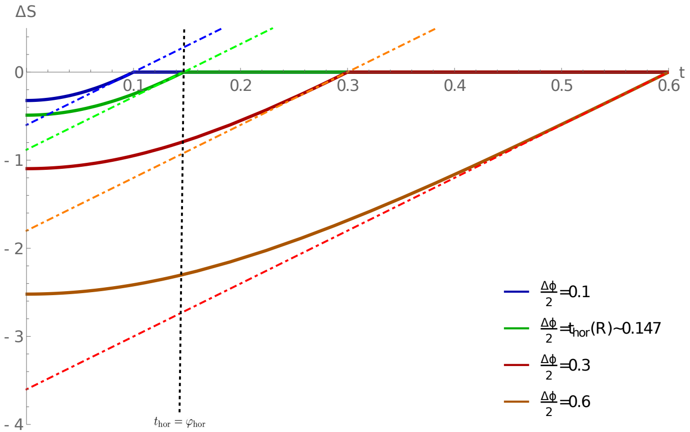

Bound on size of segments which probe the interior:
$\frac{\Delta\varphi}{2} \geq \varphi_{\text{hor}} = \frac{1}{2R} \operatorname{arcsinh} \tanh \frac{\pi R}{2}$

Evolution of mutual information (bilocal quench)

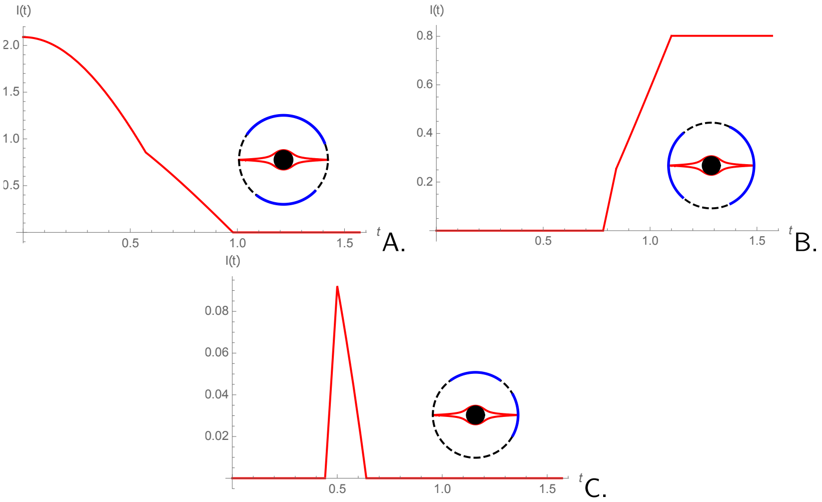

$$I(A,B) = S(A) + S(B) - S(A \cup B)$$

Evolution of mutual information (global quench)

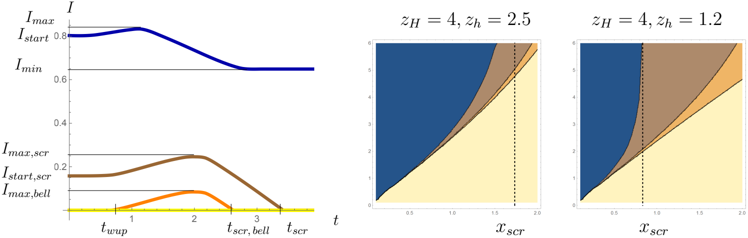

Figure: Different regimes of the MI evolution in the heating process of two disjoint intervals.

$$I(A,B) = S(A) + S(B) - S(A \cup B)$$

Evolution of MI for composite systems (global quench)

5 types of MI time dependence

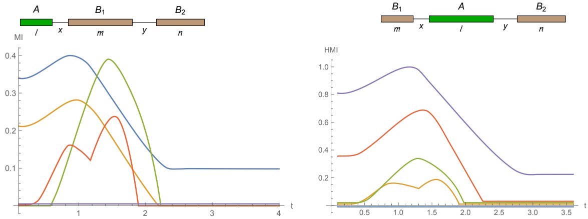

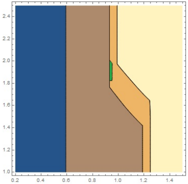

IA, O.Inozemchev, I.Volovich

Conclusions

- Non-trivial non-equilibrium dynamics are shown by susbsystems which contain one of the excitations.
- Explicit formula for non-equilibrium HEE.
- Many similarities with global quench $\Rightarrow$ more evidence for universality of entanglement growth
- Significant difference from the global quench:
  - sharp transition
  - $\phi <-> t$ symmetry
- Linear growth, loss of memory about the initial state and black hole interior are intimately connected:
  Linear growth of entanglement is a diagnostic of the information loss in the bulk
- Mutual information:
  - many possibilities;
  - "Bell"-type ("breather") in the temporal behavior.

Open questions

- CFT computation of HEE and correlation functions
- Corrections to the holographic limit (memory/information restoration?)
- Higher-dimensional generalizations
- Generalization to the n-local case (collision of n particles in the bulk)

Backup slides

Geodesic approximation for two-point boundary correlators

We are interested in the two-point correlation function of light* scalar operator $\langle \mathcal{O}_\Delta(a)\mathcal{O}_\Delta(b)\rangle$. Consider the propagator for bulk field Φ on asymptotically AdS space in the worldline representation:

$$G(a,b) = \int_{X(0)=a}^{X(1)=b} \mathcal{D}X(\lambda)\, \mathrm{e}^{im\int_0^1 d\lambda\sqrt{-g_{\mu\nu}\dot{X}^\mu\dot{X}^\nu}}, \qquad m^2 = \Delta(\Delta - d)$$

Steepest descent expansion ($m \sim \Delta \gg 0$):

$$G(a,b) \sim \sum \mathrm{e}^{-\Delta\mathcal{L}(a,b)} \tag{2}$$

Extrapolate the bulk field to the boundary: $\mathcal{O}_\Delta = \lim_{\varepsilon\to 0}\varepsilon^{-\Delta}\Phi \to$ Geodesic approximation for boundary correlators (Balasubramanian, Ross, 2000):

$$\langle \mathcal{O}_\Delta(a)\mathcal{O}_\Delta(b)\rangle = \sum \mathrm{e}^{-\Delta\mathcal{L}_{\text{ren}}(a,b)}$$

Geodesic image method

In our case there are multiple geodesics connecting two boundary points, so we have to sum over them

$$\langle \mathcal{O}_\Delta(a)\mathcal{O}_\Delta(b)\rangle = \sum \mathrm{e}^{-\Delta\mathcal{L}_{\text{ren}}(a,b)} = \sum_n Z_n(a, b^{*n})^\Delta \mathrm{e}^{-\Delta\mathcal{L}_{\text{ren}}(a,b^{*n})}$$

Sum includes direct geodesic and geodesics which wind around defects. The latter ones can be accounted for using image geodesics from point a to images of b w.r.t. identification isometry: i. e. $\mathbf{x}_{b^*} = \mathbf{u}^{-\mathbf{1}}\mathbf{x}_b\mathbf{u}$.
(D. Ageev, I. Aref'eva, M. K., M. Tikhanovskaya: 1512.03362, 1512.03363, 1604.08905)

- Consider image geodesics: $\mathcal{L}(a, b^*)$, $\mathcal{L}(a, b^{**})$, ..., $\mathcal{L}(a, b^{*n})$
- Length of a winding geodesic equals to the length of an image geodesic
- The renormalization scheme takes into account invariance with respect to identification $*$.
- Applicability of semiclassical expansion: $\mu(\epsilon) \gg \Delta \gg 0$
- The prescription is continued to the Lorentzian signature using the reflection mapping according to recipe in 1604.08905

Applicability of the geodesic prescription

- The background metric must have a well-defined Euclidean analytic continuation
- In the Lorentzian signature the prescription is viable only for spacelike-separated points on the boundary
- $0 \ll \Delta \ll \mu$. (Steepest descent and no backreaction)
- In general, one has to sum over **all** geodesics between two given boundary points
- In the general case, there is a non-perturbative contribution to the full propagator. It vanishes in the case where AdS is an orbifold (I. Aref'eva, M. K., arXiv:1601.02008)
- The renormalization scheme must be tailored for every specific deformation of AdS spacetime